Direct Modulation of Semiconductor Injection Lasers

PETER RUSSER, SENIOR MEMBER, IEEE, AND GÜNTHER ARNOLD

(Invited Paper)

Abstract—**Narrow stripe geometry double-heterostructure injection lasers for optical communication applications allow direct modulation up into the Gbit/s range. Modulation behavior and influence of modulation on the laser spectrum are discussed. The spectral and modulation properties of gain-guided and index-guided laser types differ significantly. Limitations arise from intensity fluctuations due to intrinsic quantum noise, dynamic instabilities, and reflected optical power, and also, in the case of analog modulation, from harmonic distortion. By coherent injection locking, single mode operation and strongly damped transient response can be achieved. Electronic circuits for Gbit/s direct modulation are discussed.**

I. Introduction

IN THE RAPIDLY developing field of optical communications, the semiconductor injection laser has become the most promising light source [1]–[6]. Its main advantages are simple pumping by dc current, high efficiency, and direct modulation capability up into the gigahertz range. GaAs/$Ga_xAl_{1-x}As$ lasers emit in the wavelength region of 0.8–0.9 μm and exhibit room temperature lifetimes greater than 10^6 h [7], [8]. Quaternary lasers for the wavelength region between 1.1 and 1.6 μm meet with growing interest [9]–[13], since in this region a fiber attenuation as low as 0.5 dB/km at 1.3 μm and 0.2 dB/km at 1.55 μm is possible [14]–[16]. Furthermore, monomode fibers have a dispersion minimum at 1.29 μm, yielding a pulse broadening of only 4 ps nm^{-1} km^{-1} [15].

In this paper we discuss the modulation behavior of semiconductor injection lasers for communication applications.

II. Laser Structure and Laser Operation

Modern semiconductor injection lasers for optical communications are constructed in double heterostructure (DHS) and narrow stripe geometry. By this way, low threshold currents and stable operation in the fundamental transverse mode are achieved. Fig. 1 shows the structure of a modern DHS stripe geometry GaAs/$Ga_xAl_{1-x}As$ injection laser [8], [17], the V-groove laser. The active p-GaAs layer is sandwiched by two $Ga_xAl_{1-x}As$ layers which exhibit a higher band gap than the active region. By this way, the $Ga_xAl_{1-x}As$ layers provide carrier confinement as well as an optical confinement in the vertical direction.

Manuscript received June 2, 1982.

P. Russer is with Technische Universität München, Lehrstuhl für Hochfrequenztechnik, Arcisstrasse 21, D-8000 München 2, Germany

G. Arnold is with AEG-Telefunken, Forschungsinstitut, Elisabethenstrasse 3, D-7900 Ulm, Germany.

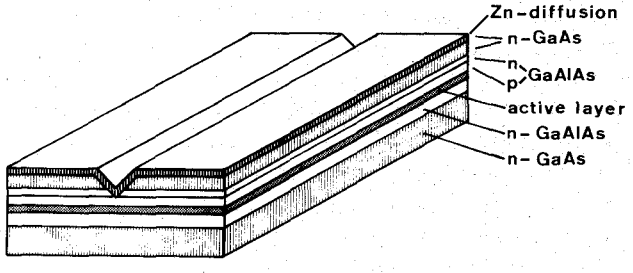

Fig. 1. V-groove laser structure.

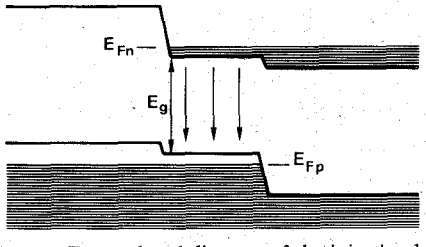

Fig. 2. Energy-band diagram of the injection laser.

The p-type $Ga_xAl_{1-x}As$ layer and a subsequent n-type $Ga_xAl_{1-x}As$ layer form an insulating pn junction. Below the etched V-groove the n-$Ga_xAl_{1-x}As$ layer is converted to p-type with a shallow Zn diffusion. In this way, a narrow conduction path approximately 3 μm wide is formed below the V-groove. The structure exhibits no refractive index variation in the plane of the active layer. Waveguiding within the junction is accomplished by gain confinement only. If a current in forward direction is impressed, electrons and holes are injected into the active region, formed by the GaAs layer. Due to the lower band gap of the GaAs layer, electrons and holes are confined within this layer. Fig. 2 shows the energy-band diagram of the injection laser. Since GaAs is a direct semiconductor, electrons and holes recombine radiatively with a high internal quantum efficiency. The cleaved laser end faces act as mirrors, so that the radiation is generated within a Fabry–Perot cavity. In the case of current injection, valence band and conduction band are in nonequilibrium and exhibit different quasi-fermi levels E_{Fp} and E_{Fn}. For a sufficiently large injection current, the separation between E_{Fp} and E_{Fn} exceeds the energy gap E_g, and an effective population inversion is established in the active region. As a consequence, the active region exhibits optical gain within a certain wavelength interval. The photons created by

0018-9480/82/1100-1809$00.75 ©1982 IEEE

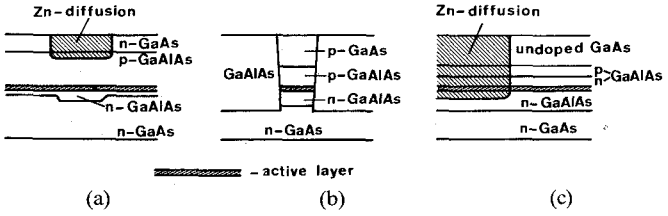

Fig. 3. Index-guided laser structures. (a) Channeled substrate planar (CSP) laser [19]. (b) Buried heterostructure (BH) laser [20]. (c) Transverse junction stripe (TJS) laser [21].

stimulated emission are in phase with the stimulating field. Furthermore, the stimulated emission rate into the modes is proportional to the number of modes in the resonator. When the laser is switched on, the spontaneous emission processes give the initial field contribution from which the photon field is built up. At a certain threshold level of the injection current the round-trip gain for the electromagnetic wave exceeds the bulk and mirror losses for a certain mode and the laser starts to oscillate.

The V-groove laser has no built-in index waveguide in the transverse horizontal direction. The oscillating mode is guided only by the gain profile within the junction plane. Other laser types with gain guiding are the oxide-stripe laser [18], the diffused-stripe laser with low diffusion, and the proton-implanted laser. Some injection laser structures exhibit index guiding also in the lateral direction. Examples of these "index-guided lasers" are the channeled substrate planar (CSP) laser [19], the diffused-stripe laser with deep diffusion, the buried-heterostructure (BH) laser [20], the transverse junction stripe laser (TJS) [21], and the constricted double-heterostructure laser [22]. Fig. 3 shows some index-guided laser structures. Examples of quaternary lasers with index guiding are the BH laser [23], the buried crescent (BC) laser [13], and the self-aligned structure laser [24]. Spectral and modulation behavior of gain-guided and index-guided lasers differ significantly.

III. The Rate Equations

The rate equations describe the dynamic behavior of a semiconductor injection laser [25]–[30]. The quantum mechanical rate equations describing the electron density and polarization and the photon amplitude give information about the time development of the amplitude, frequency, and phase of the photon field, and also about its statistical properties [25]. However, in many cases, only the time evolution of the mode intensities is of interest and one may restrict the analysis to the much simpler classical rate equations [26]–[30].

We give a discussion of the classical rate equations for the laser with N oscillating modes. The rate equations for the electron density $n(t)$ and for the photon number $S_i(t)$ in the ith mode are given by

$$\frac{dn}{dt} = \frac{J(t)}{e_0 d} - \frac{1}{\kappa} R_{sp}(n) - \sum_{i=1}^{N} \frac{K_i \Gamma_i}{V \Phi(E_i)} S_i r_{st}(E_i, n) \quad (1)$$

$$\frac{dS_i}{dt} = -\frac{S_i}{\tau_{ph_i}} + \frac{K_i \Gamma_i}{\Phi(E_i)} \left(r_{sp}(E_i, n) + S_i r_{st}(E_i, n) \right). \quad (2)$$

In (1) and (2), $J(t)$ is the injection current density, and e_0 the absolute value of the electron charge. The stimulated and spontaneous emission rates per unit of volume and unit of photon energy $r_{st}(E, n)$ and $r_{sp}(E, n)$ depend on the photon energy E and the carrier density n. V and d are volume and thickness of the active region.

Lasher and Stern have calculated r_{sp} and r_{st} for GaAs at room temperature, assuming transition between parabolic bands with k selection rule for pure material and without k selection rule for highly doped material [31]. For transitions between parabolic bands without k selection rule and analytic solution for $r_{st}(E, n)$ has been given in [32].

R_{sp} is the total spontaneous emission rate per unit of volume and follows from r_{sp} via

$$R_{sp}(n) = \int_0^\infty r_{sp}(E, n)\, dE. \quad (3)$$

For the spontaneous emission energy halfwidth ΔE_{sp} or the corresponding wavelength halfwidth $\Delta \lambda_{sp}$, respectively, we obtain approximately

$$R_{sp}(n) = r_{sp}(E_0, n) \Delta E_{sp} = r_{sp}(\lambda_0, n) \frac{c \Delta \lambda_{sp}}{\lambda_0^2} \quad (4)$$

where E_0 and λ_0 are photon energy and wavelength in the spontaneous emission maximum. With the internal quantum efficiency κ (that is, the ratio of the number of radiative spontaneous transitions to the total number of spontaneous recombination processes) we obtain the total spontaneous carrier recombination rate $1/\kappa R_{sp}$. The value of κ can be as high as 80 percent. In the linear approximation we obtain

$$\kappa^{-1} R_{sp}(n) \doteq \frac{n}{\tau_{sp}} \quad (5)$$

where τ_{sp} is the spontaneous electron lifetime. Measured values of τ_{sp} are between 2 and 8 ns for room temperature double-heterostructure GaAs lasers [33], [34].

The spontaneous and stimulated emission rates, both into the ith mode are given by $(K_i \Gamma_i / \Phi(E_i)) r_{sp}(E_i, n)$ and $(K_i \gamma_i / \Phi(E_i)) S_i r_{st}(E_i, n)$. $\Phi(E)$ is the number of orthogonal modes per unit of volume and unit of energy, Γ_i is the photon confinement factor of the ith mode and K_i is the equivalent mode number. $\Phi(E_i)$ is given by

$$\Phi(E_i) = \frac{\bar{n}_i' \bar{n}_i^2 E_i^2}{\pi^2 \hbar^3 c^3} \quad (6)$$

where $\bar{n}_i$ is the index of refraction for the ith mode, and the effective index of refraction $\bar{n}_i'$ considering the dispersion is given by

$$\bar{n}_i' = \left(1 - \frac{\lambda_i}{\bar{n}_i} \frac{d\bar{n}_i}{d\lambda} \right). \quad (7)$$

For a free-space wavelength of 8500 Å, the photon energy is $E_i = 1.46$ eV and with $\bar{n} = 3.6$ and $\bar{n}' = 5$ [35], we obtain for the number of modes per unit of volume and unit of energy $\Phi(E_i) = 1.817 \cdot 10^{12}$ meV^{-1} cm^{-3}. The photon confinement factor Γ_i gives the ratio of photon energy concentrated within the active layer of volume V to the total photon energy, both for the ith mode. For $d < 0.5$ μm, the

photon confinement factor Γ_i decreases considerably with d. For $d = 0.2$ μm, we obtain $\Gamma_i = 0.6$ [36], [37]. The equivalent mode number K_i plays an important role for lasers of the gain-guiding type [38]. For any mode of an orthogonal mode family, the near-field area A_i and the far-field solid angle Ω_i fulfill the relation $A_i\Omega_i = \lambda_i^2$ [39]. For nonorthogonal modes, the product $A_i\Omega_i$ can exceed the value λ_i^2 and the factor

$$K_i = \frac{A_i\Omega_i}{\lambda_i^2} \tag{8}$$

denotes the number of orthogonal modes to which the nonorthogonal mode is equivalent in the phase space. Index-guided lasers have orthogonal modes and, therefore, $K_i = 1$. Gain-guided lasers exhibit index guiding only in the transverse direction. We obtain, therefore, K_i from the product of the lateral near-field halfwidth w_i and the far-field angle γ_i

$$K_i = \frac{w_i\gamma_i}{\lambda_i}. \tag{9}$$

For a typical V-groove laser, $K = 11$ has been calculated [38] and values up to $K = 100$ seem to be possible for narrow stripe geometry gain-guided lasers [40]. Measured values of K are between 15 and 25.

The ratio α_i of the spontaneous processes radiating into the ith mode, $(K_i\Gamma_i/\Phi(E_i))r_{sp}(E_i, n)$ to the total number of spontaneous recombination processes per unit of time $V\kappa^{-1}R_{sp}(n)$ is given by

$$\alpha_i = \frac{\kappa K_i\Gamma_i}{V\Phi(E_i)\Delta E_{sp}}. \tag{10}$$

For GaAs lasers, ΔE_{sp} is approximately 50 meV.

For $\Phi(E) = 1.817 \cdot 10^{12}$ meV^{-1} cm^{-3}, an internal quantum efficiency of $\kappa = 0.8$, an active region of 0.2-μm thickness, 250-μm length, 3-μm width, and a corresponding $\Gamma_i = 0.6$, we obtain $\alpha_i \doteq 3.5 \cdot 10^{-5}$ for lasers with index guiding. Gain guiding may increase α by more than one order of magnitude. The photon lifetime in the ith mode is given by [26], [35]

$$\tau_{ph_i} = \frac{\bar{n}_i'}{c}\left(\alpha_i' + \frac{1}{L}\ln\frac{1}{R_i}\right)^{-1} \tag{11}$$

with the internal loss per unit length α_i, the laser end mirror reflectivity R_i, and the laser length L. For $\alpha_i' = 10$ cm^{-1}, $R_i = 0.3$ [35], $\bar{n}_i' = 5$, and $L = 250$ μm, we obtain $\tau_{ph} = 2.9$ ps.

III. The Stationary Operation

At the laser threshold for one mode the gain from the stimulated emission processes equals the losses. From (2) we obtain

$$\frac{1}{\tau_{ph_0}} = \frac{K_0\Gamma_0}{\Phi(E_0)}r_{st}(E_0, n_{th}) \tag{12}$$

for the threshold electron density n_{th}. The index 0 denotes the mode with the lowest threshold. Neglecting the α_i for small α_i we obtain from (1) and (5) the threshold current density

$$J_{th} = \frac{e_0 dn_{th}}{\tau_{sp}}. \tag{13}$$

This definition of the threshold current density is also used for gain-guided laser types which exhibit a considerable increase of radiation already at threshold. If $\alpha_0 \doteq 0$, i.e., if the spontaneous emission into the lasing mode can be disregarded, (12), in the steady-state, has to be fulfilled also above threshold. From (1), (5), (12), and (13) we obtain the photon number of the lasing mode

$$S_0 = \frac{Vn_{th}\tau_{ph}}{\tau_{sp}}\left(\frac{J}{J_{th}} - 1\right). \tag{14}$$

In the limit of $\alpha \doteq 0$, only the laser mode with the lowest threshold carrier density n_{th} oscillates. Furthermore, in this case, the photon number linearly depends on the injection current density J_{th}. However, for a high frequency direct laser modulation we cannot expect a linear dependence of the light intensity on the injection current.

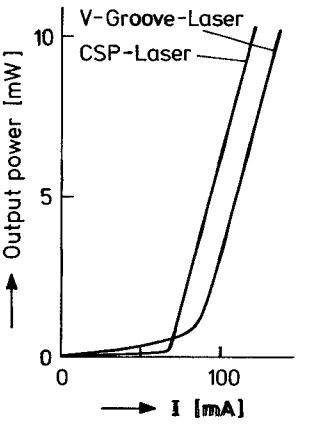

Fig. 4. Light output versus injection-current characteristics of a CSP laser and a V-groove laser.

Fig. 4 shows the dc light output versus injection current characteristics of a CSP laser and a V-groove laser. The CSP laser, which has a low α_i in the order of some 10^{-5}, exhibits only small increase of the light output power below threshold, whereas the gain-guided V-groove laser shows a smooth transition from the luminescent region into the lasing state. This smooth transition is due to the spontaneous emission term in (1). From (1) and (10) we obtain in the steady-state

$$S_i = \alpha_i nV\frac{\tau_{ph_i}}{\tau_{sp}}\left[1 - \tau_{ph_i}\frac{K_i\Gamma_i}{\Phi(E_i)}r_{st}(E_i, n)\right]^{-1}. \tag{15}$$

For $\alpha_i \neq 0$ in the steady-state n will be below the n_{th} given by (12). From (15) it follows that for $\alpha_i = 0$ only one mode, for which the term in the bracket of (15) vanishes, may exist. For $\alpha_i \neq 0$ several modes will exist. Fig. 5 shows the steady-state spectra of a CSP laser and a V-groove laser. The CSP laser oscillates in a single longitudinal mode, whereas the V-groove laser due to its higher spontaneous emission spectrum oscillates in several longitudinal modes.

Due to narrow stripe geometries, the modern laser types oscillate in the fundamental transverse mode, and exhibit

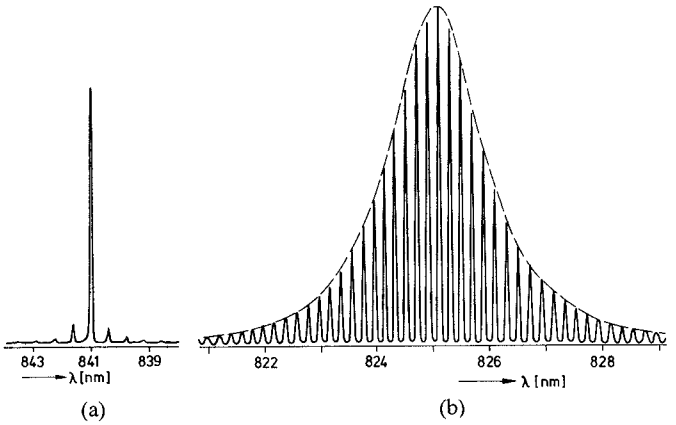

Fig. 5. Steady-state spectra of (a) a CSP laser and (b) a V-groove laser, both at 5-mW optical power.

no so-called "kinks" in the light output versus current characteristics [2], [40]–[42]. The fundamental transverse mode exhibits a longitudinal mode group with a wavelength separation $\delta\lambda$ of adjacent modes, given by [34]

$$\delta\lambda = \frac{\lambda_i^2}{2L\bar{n}_i'}. \tag{16}$$

For GaAs lasers with a typical length of 200–400 μm, the longitudinal modes are separated by 1.5–3 Å. The spectral position of the lasing modes is very sensitive to temperature changes [43]. Since the band gap of a semiconductor decreases with increasing temperature, the wavelength of maximum gain also increases. For GaAs, this temperature coefficient is approximately 2.5 Å/K. The wavelength of an individual spectral mode also has a temperature coefficient because of the temperature dependence of the refractive index of the semiconductor. For GaAs, this temperature coefficient is approximately 0.4 Å/K [44].

IV. Direct Modulation of Injection Lasers

For the analysis of the rate equations we introduce the normalized electron density $z = n/n_{\text{th}}$, the normalized photon number $x_i = S_i\tau_{\text{sp}}/Vn_{\text{th}}\tau_{\text{ph}_0}$, the normalized injection current $\eta = J/J_{\text{th}}$, and the normalized gain $g_i(z) = r_{\text{st}}(E_i, n)/r_{\text{st}}(E_0, n_{\text{th}})$, and obtain the normalized rate equations

$$\tau_{\text{sp}}\frac{dz}{dt} = \eta - z - \sum_i x_i g_i(z) \tag{17}$$

$$\tau_{\text{ph}_i}\frac{dx_i}{dt} = x_i[g_i(z) - 1] + \alpha_i z. \tag{18}$$

In the gain maximum, the approximation

$$g_0(z) = z^l \tag{19}$$

can be used with $l = 3$ for GaAs DHS lasers at room temperature [28]. The Taylor expansion of the gain around the gain maximum yields a square-law dependence of gain on the wavelength. Therefore, the normalized gain of the ith mode is given by [30]

$$g_i(z) = g_0(z)(l - \epsilon i^2). \tag{20}$$

For a gain linewidth of 120 Å and a mode spacing $\delta\lambda = 2$ Å, the coefficient ϵ is in the order of 10^{-3}.

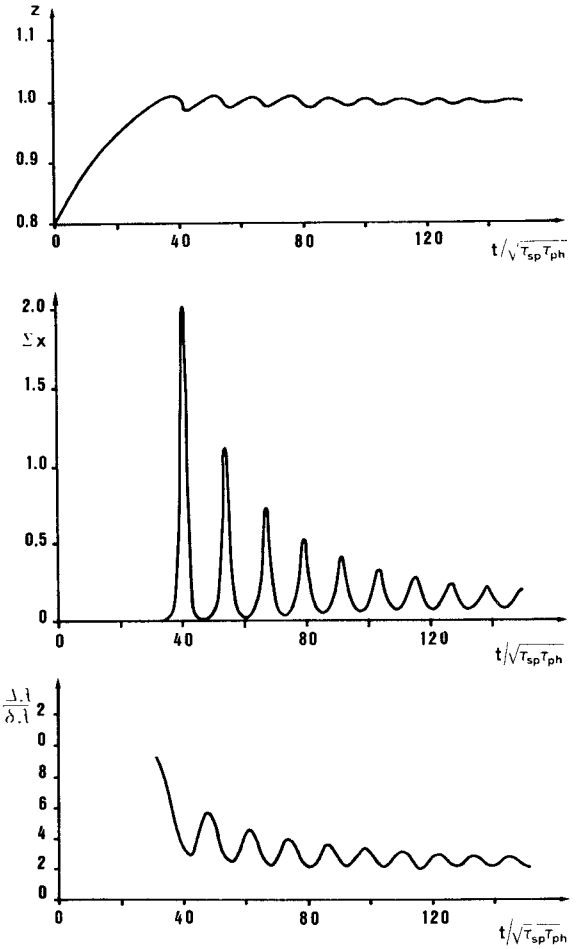

Fig. 6. Transient response of an injection laser initially biased below threshold ($\eta = 0.8$) when the current is switched to $\eta = 1.1$ at $t = 0$ for $\tau_{\text{sp}}\tau_{\text{ph}} = 900$, $\alpha = 10^{-5}$, $l = 3$, and $\epsilon = 10^{-3}$.

Fig. 6 shows the calculated transient response of an injection laser to a step current pulse with the normalized amplitude $\eta = 1.1$. The calculations have been performed for 21 modes. The laser parameters are $\tau_{\text{sp}}/\tau_{\text{ph}} = 900$, $\alpha = 10^{-5}$. We have chosen $l = 3$ and $\epsilon = 10^{-3}$ for all calculations. The spectral width $\Delta\lambda$ of the laser is given by

$$\Delta\lambda = 2\delta\lambda\left[\frac{\sum_i i^2 x_i}{\sum_i x_i}\right]^{1/2}. \tag{21}$$

If a step current pulse η is applied to initially unbiased laser or to a laser biased below threshold, the electron density in the active layer increases. After an initial delay time t_d the electron density reaches its threshold value. For the unbiased laser t_d is given by [46]

$$t_d = \tau_{\text{sp}}\ln[\eta/(\eta - 1)]. \tag{22}$$

If the laser is prebiased with η_0 and a step pulse of amplitude η_p is superimposed, the delay time t_d is reduced to

$$t_d = \tau_{\text{sp}}\ln[\eta_p/(\eta_p + \eta_0 - 1)]. \tag{23}$$

After the initial delay, the light intensity first increases rapidly and is then subject to damped relaxation oscillations. These relaxation oscillations are generated in the following way. When the electron density reaches its threshold value, the photon number has not yet reached its stationary value, where the stimulated processes would effect a high carrier recombination rate. Therefore, the carrier density further increases above its threshold value. The increase in the number of photons in the laser modes starts from an initial level determined by the spontaneous processes. The photon number increase is at first very slow since the rate of photon creation is proportional to the actual photon number. If the photon number passes its stationary value, due to the rapidly increasing stimulated recombination processes, the carrier density quickly decreases but the photon numbers further increase until the carrier density falls below the threshold value. Now the photon number decreases. After the photon number falls below its stationary level, the electron density increases again until the threshold carrier density is reached again. Afterwards, the whole process is repeated, but since the initial photon number now is higher than at the beginning of the process, the photon number reaches its equilibrium value at a shorter time. Therefore, the overshoot in the electron density and the following photon number overshoot are smaller than before, and the oscillations are damped. For low values of α, there is a considerable delay between the passing of the threshold level by the carrier density and the intensity maximum of the first spike. A low spontaneous emission results in a strong spiking.

For higher values of α, the transient oscillations may be aperiodic since for a higher spontaneous emission the initial photon number is reached earlier and the overshoot is smaller. Gain-guided lasers exhibit a higher value of α and oscillate in several longitudinal modes. In the multimode case, the relative contribution of spontaneous emission into the oscillating modes is proportional to the number of oscillating modes. This can result in an aperiodic transient behavior. In extremely narrow laser structures, the transient oscillations are damped due to carrier diffusion. The diffusion damping is proportional to $(L_D/s)^2$ where L_D is the diffusion length and s is the stripe width [50], [51]. For the very narrow buried heterostructure geometry the diffusion damping is equivalent to α values between 10^{-2} and 10^{-3}.

Injection lasers are well suited for digital applications up into the Gbit/s range. Fig. 7 shows the calculated light intensity and spectral width for direct modulation with a 101101 return to zero pcm signal. The laser data are $\tau_{sp}/\tau_{ph} = 900$ and $\alpha = 10^{-5}$. The laser is prebiased to threshold ($\eta_0 = 1$) and the normalized modulation signal amplitude is 0.1. The laser exhibits strong spiking during the modulation pulses. The increase of the light output power is accompanied by a decrease of the spectral width $\delta\lambda$.

Fig. 8 shows the response of an injection laser with $\alpha = 10^{-4}$ and $\tau_{sp}/\tau_{ph} = 2500$ to a nonreturn to zero signal with $\eta_0 = 1$ and a normalized modulation amplitude of 0.1.

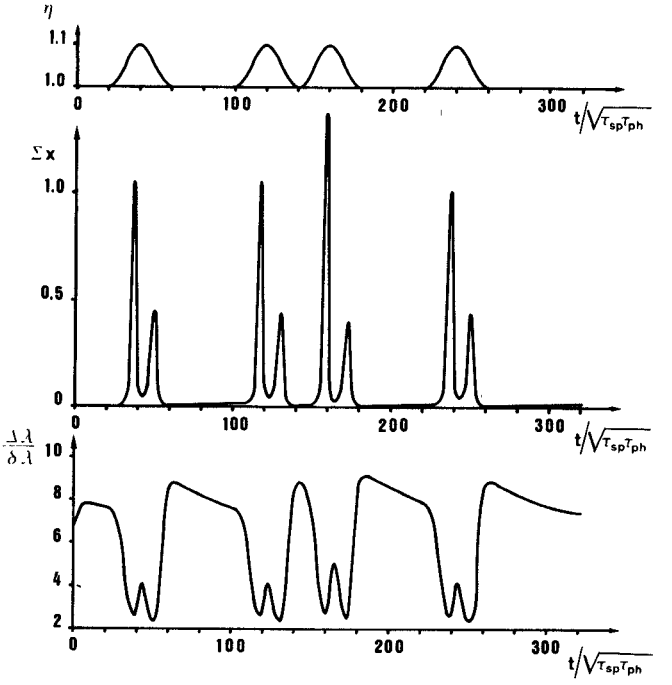

Fig. 7. Response to a *rz* pcm pattern for $\tau_{sp}/\tau_{ph} = 900$, $\alpha = 10^{-5}$, $1 = 3$, and $\epsilon = 10^{-3}$.

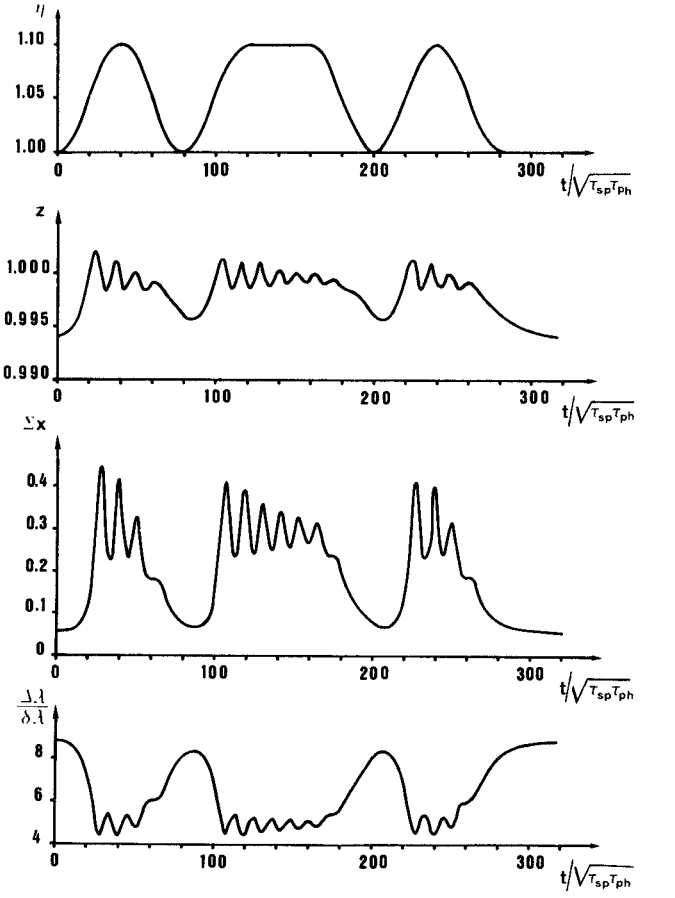

Fig. 8. Response to a *nrz* pcm pattern for $\tau_{sp}/\tau_{ph} = 2500$, $\alpha = 10^{-5}$, $1 = 3$, and $\epsilon = 10^{-3}$.

Due to the higher value of α the laser exhibits low transient ringing and higher spectral width. Increasing the bias current to $\eta_0 = 1.05$ (Fig. 9) reduces the transient ringing as

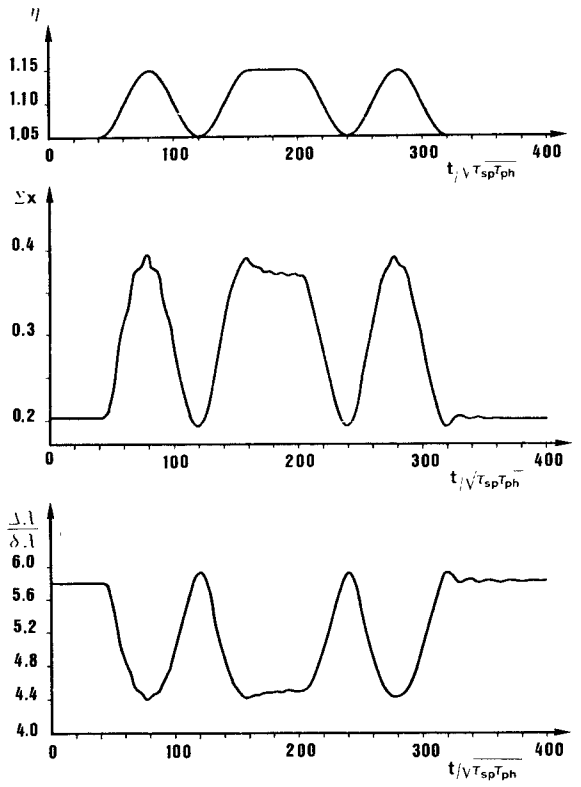

Fig. 9. Response to a *nrz* pcm pattern for $\tau_{sp}/\tau_{ph} = 2500$, $\alpha = 10^{-5}$, $I = 3$, and $\epsilon = 10^{-3}$.

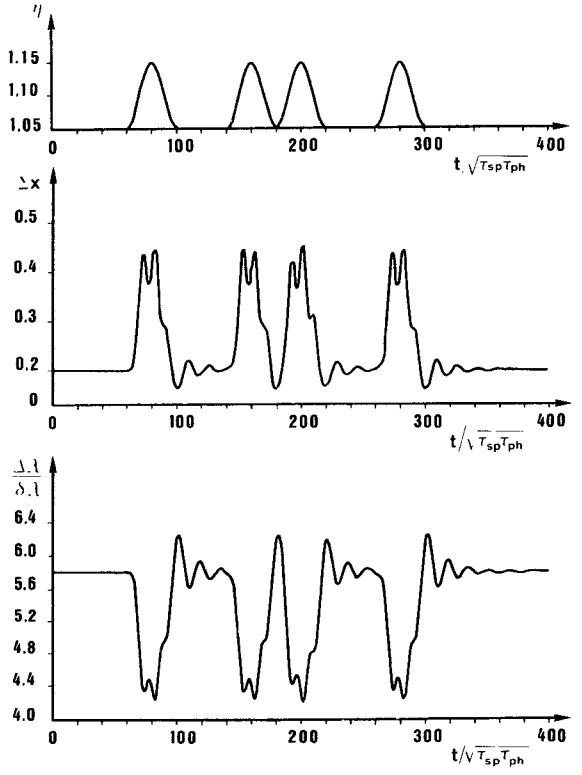

Fig. 10. Response to a *rz* pcm pattern for $\tau_{sp}/\tau_{ph} = 2500$, $\alpha = 10^{-5}$, $I = 3$, and $\epsilon = 10^{-3}$.

well as the spectral width. Fig. 10 shows the modulation behavior of the same laser and the same bias conditions for return to zero modulation. Fig. 11 shows the direct modulation of a GaAs V-groove laser with a 1-Gbit/s return to zero signal [17], and Fig. 12 shows a 280-Mbit/s pcm modulation pattern of a quaternary V-groove laser [52]. In order to obtain low pattern effects, i.e., bit pattern dependend modulation distortions at high bit rates, it is necessary to bias the laser up to threshold or above threshold. Modulation experiments with GaAs lasers up into the Gbit/s range have been reported by several authors [53]–[59]. A bit rate of 8 Gbit/s has been achieved using a TJS laser with a short spontaneous lifetime due to heavy doping in the active region [59]. With $Ga_xIn_{1-x}As_yP_{1-y}$ buried stripe lasers, modulation up to 2 Gbit/s has been carried out in the 1.3-μm wavelength region [60]–[62]. Far below threshold, injection lasers show a broad spontaneous emission spectrum with a halfwidth of approximately 300 Å. With increasing current, this spectrum is narrowed and exhibits a mode structure at and above threshold. Modern narrow stripe injection lasers oscillate only in the fundamental transverse mode. Above threshold, the width of the longitudinal mode spectrum decreases with increasing light intensity. Figs. 7–10 show also the spectral widths $\Delta\lambda$ given by (20). The spectral narrowing with increasing intensity occurs also in the dynamic case. Fig. 13 shows the calculated spectra corresponding to Fig. 9 for stationary bias at $\eta = 1.05$ and at the first light intensity maximum $t/\sqrt{\tau_{sp}\tau_{ph}} = 77$. These results are in agreement with experi-

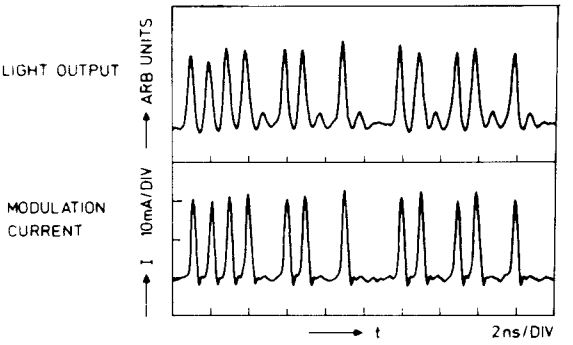

Fig. 11. Light output signal and modulation current signal of a GaAs V-groove laser modulated with a 1-Gbi/s return to zero signal [17].

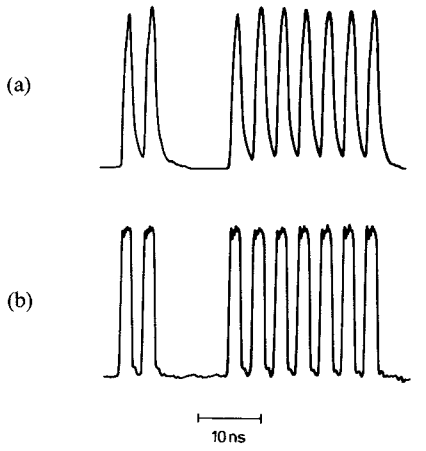

Fig. 12. (a) Light output signal and (b) modulation current signal of a $Ga_xIn_{1-x}As_yP_{1-y}$ V-groove laser with a 280-Mbit/s return to zero signal [52].

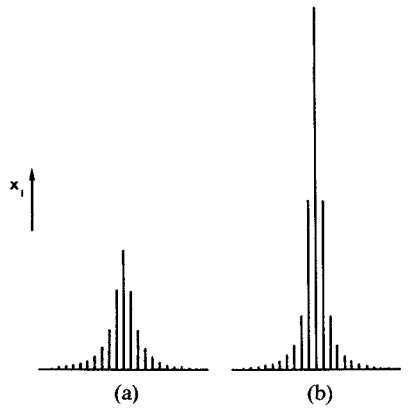

Fig. 13. Calculated emission spectra corresponding to Fig. 9, (a) for stationary bias at $\eta = 1.05$ and (b) at the first light intensity maximum $t/\sqrt{\tau_{sp}\tau_{ph}} = 77$.

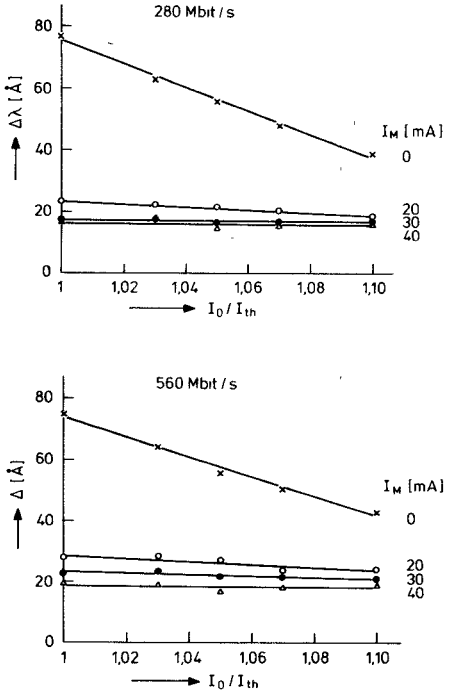

Fig. 14. Measured dependence of the spectral width $\Delta\lambda$ of a GaAs V-groove laser on the bias current I_o and on the modulation current amplitude I_M.

mental results where no significant structural change in the bias dependent CW spectra could be observed when modulating the laser [56], [57]. Fig. 14 shows the dependence of the spectral width $\Delta\lambda$ of a GaAs V-groove laser on the bias current I_o and on the modulation current amplitude I_M for modulation with 280 Mbit/s and 560 Mbit/s. The spectral broadening due to modulation reported in earlier papers [29], [63] does not occur in modern narrow stripe geometry lasers.

Sinusoidal modulation of injection lasers above threshold gives insight into the dynamic properties of injection lasers [28]–[30], [49]. For a laser biased above threshold to $\bar{\eta}$ and $\bar{x}$, respectively, and oscillating in a single-mode small signal analysis (17) and (18) yields the following dependence of the complex normalized photon amplitude $\hat{x}_1$ on the complex modulation current amplitude, both at angular

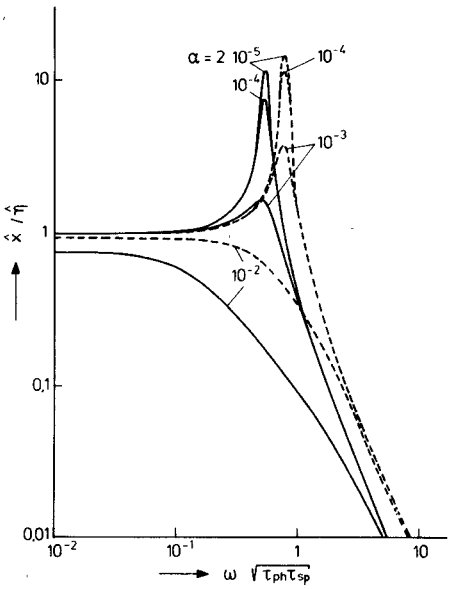

Fig. 15. Small-signal modulation depths dependence on modulation frequency for biasing 10 percent (continuous curve) and 20 percent (broken curve) above threshold for $\tau_{sp}/\tau_{ph} = 10^7$.

frequency ω:

$$\hat{x} = \frac{\bar{x}g'(\bar{z}) + \alpha}{\tau_{sp}\tau_{ph}} \frac{\hat{\eta}}{\omega_0^2 + j\omega\beta - \omega^2} \tag{24}$$

with

$$\omega_0^2 = \left[1 - g(\bar{z}) + \alpha g(\bar{z}) + x_0 g'(\bar{z})\right]/\tau_{sp}\tau_{ph} \tag{25}$$

and

$$\beta = \left[1 + \bar{x}g'(\bar{z})\right]/\tau_{sp} + \left[1 - g(\bar{z})\right]/\tau_{ph} \tag{26}$$

where $g'(\bar{z})$ denotes dg/dz. Fig. 15 shows the dependence of modulation depths on modulation frequency for biasing 10 and 20 percent above threshold for $g(\bar{z})$ given by (19) with $l = 3$ for different values of α. For $\alpha = 10^{-3}$ and smaller values of α the modulation transfer characteristic shows a resonance. The results with higher α are representative for the multimode case if an effective spontaneous emission coefficient α_{eff} is introduced [30].

For analog communication applications, semiconductor injection lasers should have low harmonic distortion even at a high modulation index. The linearity is determined from the dc light output versus current characteristic (Fig. 4) only for frequencies sufficiently below the resonance frequency ω_0 given by (25). From Figs. 7–10, where the calculations have been performed on the basis of cosine shaped modulation current pulses, we see that in the case of high frequency modulation the light output signal suffers a strong nonlinear distortion. Harth has given an analytic solution for the sinusoidal large signal modulation of injection lasers and has shown that a reduction of the modulation transfer angular resonance frequency ω_0, as well as a strong spiking, may occur [64]. Whereas at low frequencies, index-guided lasers (due to their highly linear dc light output versus current characteristic) exhibit lower modulation distortions than gain-guided laser types, at higher modulation frequencies, the gain-guided laser types show a

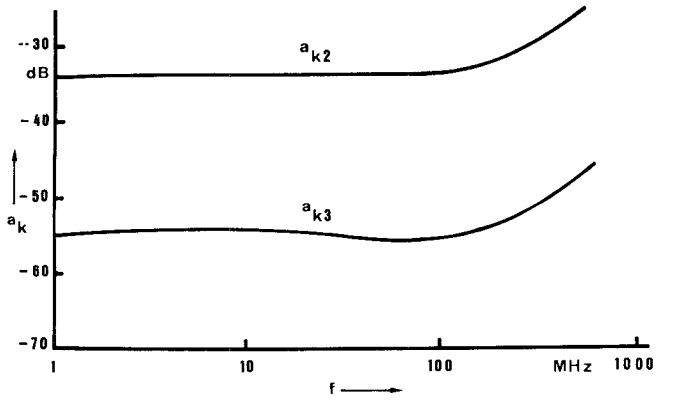

Fig. 16. Modulation frequency dependence of the second- and third-harmonic suppression a_{k2} and a_{k3} of a V-groove GaAs laser dc biased to 5-mW light output power and modulated with a modulation index $m = 0.5$ [66].

better linearity, due to the stronger damping of the nonlinear relaxation oscillations [65]. Fig. 16 shows the modulation frequency dependence of the second- and third-harmonic suppression for a V-groove GaAs laser dc biased to 5-mW light output power and modulated with a modulation index $m = 0.5$ [66]. At 1-mW optical ac power and 300-MHz modulation frequency, different laser types have shown a second-harmonic suppression between 40 and 55 dB and a third-harmonic suppression between 50 and 80 dB [67].

V. Fluctuation Phenomena

Fluctuations in the light output power of semiconductor injection lasers may impose severe limitations in the application of injection lasers. The reasons for these fluctuations are the random nature of the intrinsic quantum fluctuations, dynamic instabilities, and laser light which is reflected back in the laser diode.

The intrinsic quantum fluctuations are due to the quantum statistical nature of carrier recombination and photon generation and are unavoidable in principle [25], [68]–[71]. In an injection laser, the total light intensity of all oscillating modes is limited and, therefore, stabilized by carrier injection. Therefore, the total light intensity fluctuations are orders of magnitude smaller than the intensity fluctuations of a single mode. Fig. 17 shows the calculated noise levels at 5 MHz for index-guided and gain-guided lasers for three cases: detection of all modes, detection of the central mode intensity only, and a transmission loss that differs from mode to mode by 1 percent. Also, in the latter case, the noise level increases dramatically compared with the detection of the total light intensity. The two curves ($a1$) and ($a2$) for the index-guided lasers belong to two limiting cases when the laser exhibits one dominant mode ($a1$) and when the gain maximum of the active region is just between two modes so that the laser oscillates in two modes of equal intensity. Fig. 18 shows the measured optical carrier to noise ratio for the total light intensity of a V-groove GaAs laser for different frequencies and for a noise bandwidth of 10 MHz. The carrier-to-noise ratio increases with increasing light intensity and decreases with

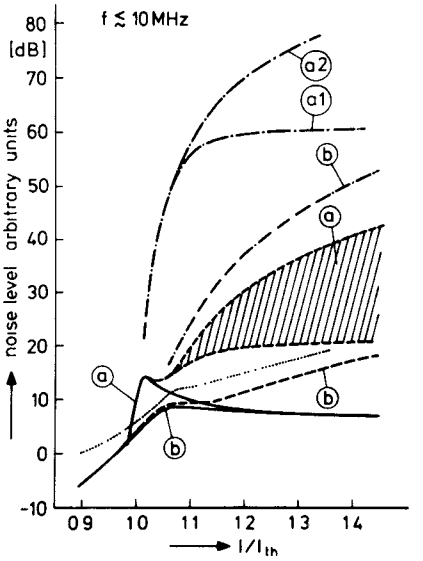

Fig. 17. Calculated noise level versus injection current in arbitrary units for uniform detection of all lasing modes (———), central mode only (- - - -), and transmission loss varying from mode to mode by 1 percent (----). Measured noise level for a V-groove laser (· · · ·) [71].

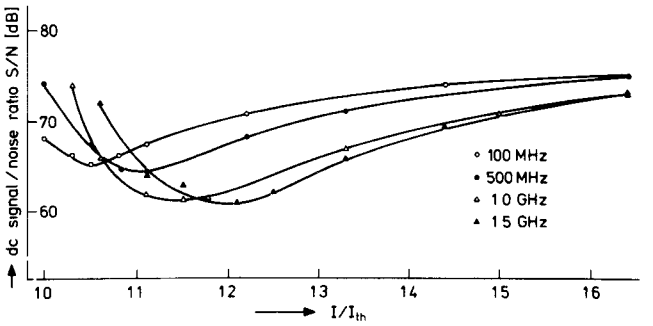

Fig. 18. Measured dc signal-to-noise ratio of a V-groove laser, prebiased to $\eta = 1.25$ for different frequencies; noise bandwidth 10 MHz [71].

increasing frequency. Due to the low spontaneous emission coefficient α, index-guided lasers may exhibit very low intrinsic quantum noise [72].

Dynamic instabilities may cause very strong intensity fluctuations. Basov supposed spatial inhomogeneities to be the reasons for dynamic instabilities [73]. If the laser resonator, for example, has two sections (one of which has optical gain and the other is lossy) in the lossy section the photon field will raise the carrier density, whereas the carrier density of the amplifying section will be lowered by the photon field. Basov has shown that the steady-state solution of the laser rate equations becomes unstable if the absorbing section saturates faster than the amplifying one. Kobayashi has shown experimentally and theoretically that stationary pulsations can arise when two parallel lasers are optically coupled [74]. In the same way, self pulsations could also be caused by the coupling of two filaments in multifilamentary injection lasers [75]. These oscillations were strongly related to the "kinks" in the light output versus current characteristics, which occurred during a change in the lasing filament. Modern narrow stripe geometry injection lasers oscillate in a single and stable transverse mode and don't exhibit this kind of instability.

However, it has also been shown that for narrow stripe injection lasers a dynamic instability may occur if the stripe width is smaller than five times the diffusion length [76], [77].

Strong intensity fluctuations also may occur if laser light is reflected back into the laser [78]–[82]. If the laser is coupled to an optical fiber, light is reflected due to Rayleigh backscattering from the fiber, and due to fiber discontinuities. The reflected light fluctuates in phase due to mechanical fiber vibration and other random influences. On the other hand, the laser diode also may suffer random frequency variations during the round trip time of the reflected light. As a consequence, the reflected light of random phase causes intensity and frequency variations in the laser diode. The sensitivity to optical feedback depends on the coherence length of the laser radiation. Gain-guided lasers exhibit a coherence length in the order of only 100 μm, whereas the coherence length of index-guided lasers is in the order of several meters. Therefore, gain-guided lasers are less sensitive to optical reflection. For high quality optical communication applications, a reflection with respect to intensity of about $10^{-3} \cdots 10^{-5}$ can be tolerated for multimode gain-guided lasers, while a reflection of only about $10^{-6} \cdots 10^{-7}$ may be tolerated for index-guided lasers [84], [85]. Multimode fibers in optical communication systems may typically exhibit a reflection in the order of 10^{-5}. Therefore, gain-guided lasers may be used in connection with multimode fibers. In the case of index-guided lasers, an optical isolator will be necessary in order to avoid fluctuations due to optical feedback.

VI. Injection Locking

The direct modulation behavior of injection lasers can be improved by injecting coherent light into an oscillating mode of the modulated laser [85]–[90]. We have seen that a high initial photon number in the oscillating modes due to a high spontaneous emission coefficient yields a strong damping of the relaxation oscillations. By injection of a coherent light signal into an oscillating mode of an injection laser, this strong reduction occurs without multimode operation. The suppression of the nonirradiated modes results from the reduction of the electron density and the associated gain caused by the light injection. Practically, coherent light injection at the center wavelength of a mode is impossible and there is always a detuning between the wavelength of the injected radiation and the wavelength of the free-running laser mode. The locking range for synchronization to the wavelength of injected radiation is proportional to the amplitude ratio of injected radiation and radiation produced in the laser and is inversely proportional to the laser length [88], [90]. For an amplitude ratio of 10^{-2}, a locking range of more than 0.1 Å can be achieved [90]. In the case of practical applications of this method, therefore, difficulties arise from the need of a very exact spectral tuning of the modulated laser to another laser which acts as a coherent light source. To overcome this difficulty, Lang and Kobayashi used two lasers with slightly different length and, therefore, slightly different

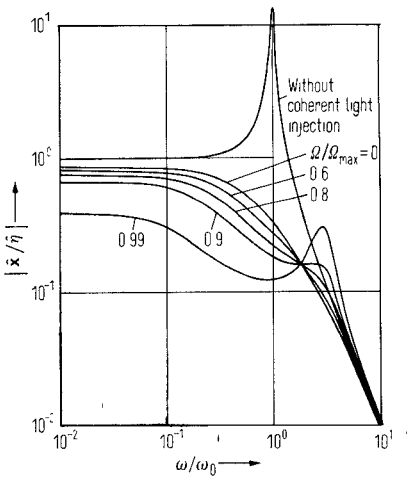

Fig. 19. Small-signal modulation depths versus modulation frequency characteristic with and without coherent light injection for different ratios of the wavelength detuning range to the wavelength locking range $\Delta\lambda_{max}$ ($\tau_{sp}/\tau_{ph}=10^3$, $1=3$, $\eta_0=1.1$).

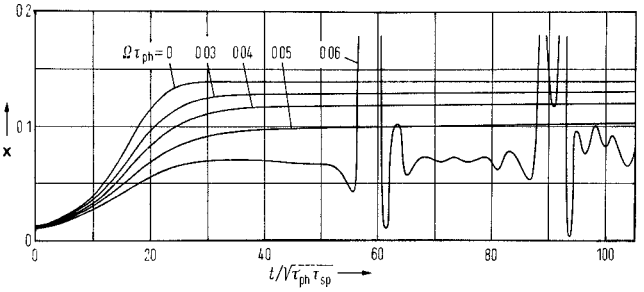

Fig. 20. Large-signal response to a step current pulse with coherent light injection. The light injection intensity corresponds to a maximum locking range $\Omega\tau_{ph}=0.05$ ($\tau_{sp}/\tau_{ph}=10^3$, $1=3$).

mode spacing [86], [88]. By appropriate choice of the laser parameters there always exist one or more pairs of modes with sufficiently close wavelengths to insure locking.

Fig. 19 shows the small-signal modulation depths versus modulation frequency characteristics with and without coherent light injection [90]. In the case of coherent light injection, different detuning $\Delta\lambda$ between the wavelength of the injected radiation and the free-running laser wavelength has been taken into consideration. Within the locking range $\pm\Delta\lambda_{max}$, the resonance in the modulation characteristic vanishes. Fig. 20 shows the large scale response to a step pulse which changes η from 0.9 to 1.1 at the time $t=0$. The light intensity corresponds to a maximum locking frequency range $\Omega\tau_{ph}=0.05$. Fig. 21 shows the light output for the same step current pulse for different normalized injection levels P_{ext} and without detuning. The normalized injection level $P_{ext}=10^{-3}$ corresponds to the injection level assumed in Fig. 22. With coherent light injection the light output power response to injection current is strongly damped within the whole locking range and exhibits no spiking response. For a detuning larger than the stationary locking range, the frequency locking breaks down and the laser produces strong spiking oscillations (Fig. 20). The frequency of these spiking oscillations is identical with the difference between the optical frequencies of the incident radiation and the unlocked laser.

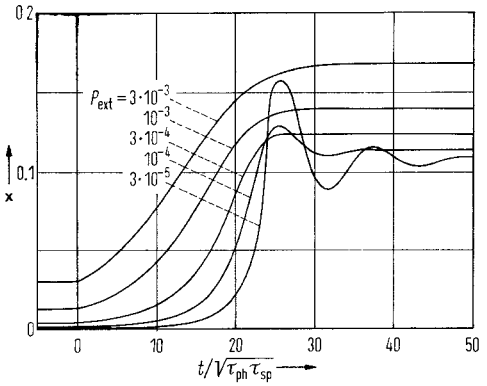

Fig. 21. Large-signal response to a step current pulse without detuning for different levels of coherent light injection ($\tau_{sp}/\tau_{ph} = 10^3$, $l = 3$).

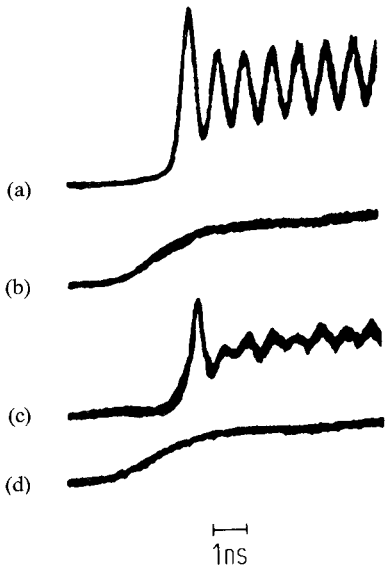

Fig. 22. Measured light output response of a laser modulated by a step current pulse with an amplitude approximately 9 percent above threshold (a) without and (b)–(d) with coherent light injection. The injecting laser was dc operated 11 percent above threshold at different heat sink temperatures (b) $T = 24°C$, (c) $T = 25°C$, and (d) $T = 26°C$.

Further injection locking experiments are reported in [91], [92]. If the difficulty of the wavelength matching of the modulated laser to the injected coherent light signal can be overcome by using a laser amplifier without reflecting mirrors, injection locking could be an interesting method for high-frequency optical modulation.

VII. Modulation Circuits

For high bit rate direct modulation of injection lasers, multiplexer and laser driver circuits are needed. Electronic circuits up into the Gbit/s range can be realized using bipolar transistors, GaAs MESFET's, Gunn effect digital devices, Schottky diodes, and step recovery diodes as the amplifying and switching devices [93]–[106]. Fig. 23 shows the circuit diagram of a hybrid integrated laser driver using bipolar transistors [96]–[98]. Control of the bias current and the modulation amplitude is possible in order to compensate for changes in the threshold current and in the slope of the light output versus current characteristic of the laser over long periods of operation. The input stage with

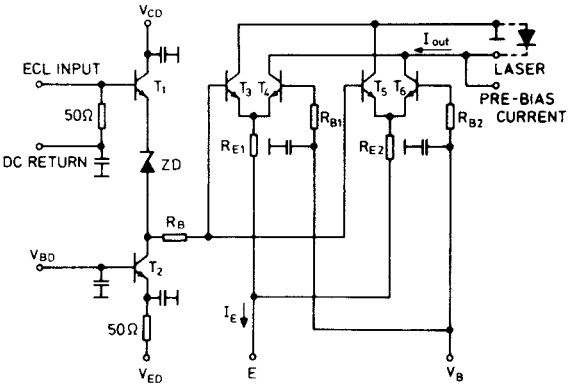

Fig. 23. Circuit diagram of the laser driver.

T_1 and T_2 provides 50-Ω input impedance and level compatibility with emitter coupled logic. The output current amplitude is controlled by a dc control current I_E fed to the differential amplifiers, the output current amplitude is independent of the input signal amplitude, and also has a faster rise time. The output amplitude can be controlled in the range from 0 to 60 mA. Using transistors with 8-GHz cutoff frequency, switching times under 200 ps (between 10 and 90 percent) were achieved with a 50-mA output amplitude. Fig. 11 shows the output current waveform of the driver, and the light output signal of the laser for an 1-Gbit/s *rz* modulation signal.

Laser control circuits for stabilization of the laser light output signal against the influence of temperature changes and degradation monitor the light output from the rear face of the laser [96], [107], [108].

VIII. Conclusion

Modern narrow stripe DHS semiconductor injection lasers exhibit a stable operation in the fundamental transverse mode and linear CW light output versus current characteristics. Direct modulation up into the gigahertz range is possible and has in general no considerable influence on spectrum and near-field. Harmonic distortions, occurring especially at high modulation frequencies, limit the application for high-bandwidth high-quality analog communications. With respect to fluctuations, the application of gain-guided laser types in connection with multimode fibers is not problematic, but the combination of index-guided lasers with monomode fibers will make necessary the use of an optical isolator. The modulation behavior may be further improved by injection locking, but this method is not yet ready for technical applications.

Acknowledgment

The authors wish to thank Dr. K.-H. Türkner for a critical reading of the manuscript.

References

[1] K. Shirahata, W. Susaki, H. Namizaki, "Recent developments in fiber optic devices," *IEEE Trans. Microwave Theory Tech.*, vol. MTT-30, pp. 121–131, Feb. 1982.

[2] M. J. Howes and D. V. Morgan, Eds., *Optical Fibre Communications*. New York: Wiley, 1980.

[3] M. Nakamura and S. Tsuji, "Single-mode injection lasers for optical fiber communications," *IEEE J. Quantum Electron.*, vol. QE-17, pp. 994–1005, June, 1981.
[4] H. Kressel and J. K. Butler, *Semiconductor Lasers and Heterojunction LED's*. New York: Academic Press, 1977.
[5] G. H. B. Thompson, *Physics of Semiconductor Laser Devices*. New York: Wiley, 1980.
[6] H. Kressel, Ed., *Semiconductor Devices*. New York: Springer, 1982.
[7] S. Nita, H. Namizaki, S. Takamiya, and W. Susaki, "Single-mode junction-up TJS lasers with estimated lifetime of 10^6 hours," *IEEE J. Quantum Electron.*, vol. QE-15, pp. 1208–1209, Nov. 1979.
[8] G. Arnold, F.-J. Berlec, G. Glasmachers, and H.-P. Vollmer, "Long-term behavior of V-groove lasers at elevated temperature," *IEEE J. Quantum Electron.*, vol. QE-17, pp. 759–762, May 1981.
[9] S. Arai, Y. Suematsu, and Y. Itaya, "1.11–1.67-μm (100) GaInAsP/InP injection lasers prepared by liquid-phase epitaxy," *IEEE J. Quantum Electron.*, vol. QE-16, pp. 197–205, Feb. 1980.
[10] D. Renner and G. Henshall, "Narrow-stripe injection lasers in GaInAsP/InP," *IEEE J. Quantum Electron.*, vol. QE-17, pp. 199–202, Feb. 1981.
[11] R. J. Nelson, R. B. Wilson, P. D. Wright, P. A. Barnes, and N. K. Dutta, "CW electrooptical properties of InGaAsP ($\lambda = 1.3$ μm) buried-heterostructure lasers," *IEEE J. Quantum Electron.*, vol. QE-17, pp. 202–207, Feb. 1981.
[12] S. Arai, M. Asada, T. Taulun-ek, Y. Suematsu, Y. Itaya, and K. Kishino, "1.6-μm wavelength GaInAsP/InP BH lasers," *IEEE J. Quantum Electron.*, vol. QE-17, pp. 640–645, May 1981.
[13] E. Oomura, T. Murotani, H. Higuchi, H. Namizaki, and W. Susaki, "Low threshold InGaAsP/InP buried crescent laser with double current confinement structure," *IEEE J. Quantum Electron.*, vol. QE-17, pp. 646–650, May 1981.
[14] A. Kawana, T. Miyashita, M. Nakahara, M. Kawachi, and T. Hosaka, "Fabrication of low-loss single-mode fibres," *Electron. Lett.*, vol. 13, pp. 188–189, 1977.
[15] N. Niizeki, "Single-mode fiber at zero-dispersion wavelength," *Dig. Topical Meeting on Integrated Optics and Guided-Wave Optics*, (Salt Lake City), Jan. 16–18, 1978, pp. MB 1-1-4.
[16] T. Miya, Y. Terumuna, T. Hosaka, and T. Miyashita, "Ultimate low-loss single-mode fibre at 1.55 μm," *Electron. Lett.*, vol. 15, pp. 106–108, Feb. 15, 1979.
[17] P. Marschall, E. Schlosser, and C. Wölk, "A new type of diffused stripe geometry injection laser," in *Supplement to the Proc. 4th Europ. Conf. Optical Communication*, (Geneva), pp. 94–97, Sept. 12–15, 1978.
[18] J. C. Dyment, L. A. D'Asaro, and T. L. Poole, "Stripe-geometry double heterostructure lasers: Mode structure and CW operation above room temperature," *Appl. Phys. Lett.*, vol. 18, pp. 155–000, 1971.
[19] K. Aiki, M. Nakamura, T. Kuroda, and J. Umeda, "Channeled-substrate-planar structure (AlGa)As diode lasers," *Appl. Phys. Lett.*, vol. 48, pp. 649–671, June 1977.
[20] T. Tsukada, "GaAs-$Ga_{1-x}Al_xAs$ buried-heterostructure injection lasers," *J. Appl. Phys.*, vol. 45, pp. 4899–4909, Nov. 1974.
[21] H. Namizaki, "Transverse-junction-stripe lasers with a GaAs p-n junction," *IEEE J. Quantum Electron.*, vol. QE-11, pp. 427–431, July 1975.
[22] D. Botez, "CW high-power single-mode operation of constricted double-heterojunction AlGaAs lasers with a large optical cavity," *Appl. Phys. Lett.*, vol. 36, pp. 190–92, 1980.
[23] H. Kano and K. Sugiyama, "Operation characteristics of buried-stripe GaInAsP/InP DH lasers made by melt-back method," *J. Appl. Phys.*, vol. 51, pp. 4539–4540, Aug. 1980.
[24] M. Yano, H. Nishi, and M. Takusagawa, "Oscillation characteristics in InGaAsP/InP DH lasers with self-aligned structure," *IEEE J. Quantum Electron.*, vol. QE-15, pp. 1388–1394, Dec. 1979.
[25] H. Haug, "Quantum-mechanical rate equations for semiconductor lasers," *Phys. Rev.*, vol. 184, pp. 338–348, 1969.
[26] J. Vilms, L. Wandinger, and K. L. Klohn, "Optimization of the gallium arsenide injection laser for maximum CW power output," *IEEE J. Quantum Electron.*, vol. QE-2, pp. 80–83, April 1966.
[27] M. J. Adams and P. T. Landsberg, "The theory of the injection laser," in *GaAs Lasers*, C. H. Gooch, Ed. London, Wiley, 1969.
[28] M. J. Adams, "Rate equations and transient phenomena in semiconductor lasers," *Opto-Electron.*, vol. 5, pp. 201–205, 1973.
[29] G. Arnold and P. Russer, "Modulation behaviour of semiconductor injection lasers," *Appl. Phys.*, vol. 14, pp. 255–268, 1977; expanded and updated treatment in *Topics in Applied Physics*, vol. 39, pp. 213–243, 1982.
[30] K. Petermann, "Theoretical analysis of spectral modulation behaviour of semiconductor injection lasers," *Optical and Quantum Electronics*, vol. 10, pp. 233–242, 1978.
[31] G. Lasher and F. Stern, "Spontaneous and stimulated recombination radiation in semiconductors," *Phys. Rev.*, vol. 133, pp. A 553–A 563, 1964.
[32] P. Russer, "Evaluation of the stimulated emission rate of semiconductors with no k selection rule," Wissenschaftliche Berichte AEG-Telefunken, pp. 167–169, 1980.
[33] J. C. Dyment, J. E. Ripper, and T. P. Lee, "Measurement and interpretation of long spontaneous lifetimes in double heterostructure lasers," *J. Appl. Phys.*, vol. 43, pp. 452–457, 1972.
[34] J. Angerstein and D. Siemsen, "Modulation characteristics of injection lasers including spontaneous emission—Part 2: Experiments," Arch. Elek. Übertragung., vol. 30, pp. 477–480, Dec. 1976.
[35] T. H. Zachos and J. E. Ripper, "Resonant modes of GaAs junction lasers," *IEEE J. Quantum Electron.*, vol. QE-5, pp. 29–37, Jan. 1969.
[36] M. B. Panish, "Heterostructure injection lasers," *Proc. IEEE*, vol. 63, pp. 1512–1540, Oct. 1976.
[37] J. K. Butler and H. Kressel, "Design curves for double-heterostructure laser diodes," *RCA Rev.*, vol. 38, pp. 542–558, Dec. 1977.
[38] K. Petermann, "Calculated spontaneous emission factor for double-heterostructure injection lasers with gain-induced waveguiding," *IEEE J. Quantum Electron.*, vol. QE-15, pp. 566–570, July 1979.
[39] G. Grau, Optische Nachrichtentechnik. Berlin: Springer, 1981, p. 156.
[40] W. Streifer, D. R. Scifres, and R. D. Burnham, "Spontaneous emission factor of narrow-stripe gain-guided diode lasers," *Electron. Lett.*, vol. 17, pp. 933–934, Nov. 1981.
[41] N. Chinone, "Nonlinearity in power output-current characteristics of stripe geometry injection lasers," *J. Appl. Phys.*, vol. 48, pp. 3237–3247, Aug. 1977.
[42] J. Buus, "Multimode field theory explanation of kinks in the characteristics of DH lasers," *Electron. Lett.*, vol. 14, pp. 127–128, Mar. 1978.
[43] M. Nakamura, "Single-mode operation of semiconductor injection lasers," *IEEE Trans. Circuits Syst.*, vol. CAS-26, pp. 1055–1065, Dec. 1979.
[44] I. Hayashi, "Recent progress in semiconductor lasers—CW GaAs lasers are now ready for new applications," *Appl. Phys.*, vol. 5, pp. 25–36, 1974.
[45] C. H. Gooch, *Injection Electroluminescent Devices*. London: Wiley, 1973, p. 138.
[46] K. Konnerth and C. Lanza, "Delay between current pulse and light emission of a gallium arsenide injection laser," *Appl. Phys. Lett.*, vol. 4, pp. 120–121, Apr. 1964.
[47] T. Ikegami, K. Kobayashi, and Y. Suematsu, "Transient behaviour of semiconductor injection lasers," *Electron. Commun. Jap.*, vol. 53-B, pp. 82–89, 1970.
[48] T. Ozeki and T. Ito, "Pulse modulation of DH-(GaAl)As lasers," *IEEE J. Quantum Electron.*, vol. QE-9, pp. 1098–1101, Nov. 1973.
[49] W. Harth and D. Siemsen, "Modulation characteristics of injection lasers including spontaneous emission–Part 1: Theory," *Arch. Elek. Übertragung.*, vol. 30, pp. 343–348, Sept. 1976.
[50] P. M. Boers, M. T. Vlaardingerbroek, and M. Danielsen, "Dynamic behavior of semiconductor lasers," *Electron. Lett.*, vol. 11, pp. 206–208, May 1975.
[51] K. Furuya, Y. Suematsu, and T. Hong, "Reduction of resonance-like peak in direct modulation due to carrier diffusion in injection lasers," *Appl. Opt.*, vol. 17, pp. 1949–1952, June 1978.
[52] P. Marschall, W. Pfister, and E. Schlosser, "New narrow diffusion-type GaInAs/InP injection laser for 1.3 μm," in *Tech. Dig. Optical Fiber Communication Conf.*, (Phoenix), pp. 50–51, April 13–15, 1982.
[53] P. Russer and S. Schulz, "Direkte Modulation eines Doppelheterostrukturlasers mit einer Bitrate von 2.3 Gbit/s," *Arch. Elek. Übertragung.*, vol. 27, pp. 193–195, Apr. 1973.
[54] M. Maeda, K. Nagano, I. Ikushima, M. Tanaka, K. Saito, and R. Ito, "Buried-heterostructure lasers for wideband linear optical sources," in *Proc. 3rd Europ. Conf. Optical Communication*, (München), pp. 120–122, Sept. 14–16, 1977.
[55] M. Nakamura, K. Aiki, J. Umeda, N. Chinone, R. Ito, and H.

Nakashima, "Single-transverse-mode low-noise (GaAl)As lasers with channeled substrate planar structure," in *Proc. Int. Conf. Integrated Optics and Optical Fiber Communication*, (Tokyo), pp. 83–86, July 18–20, 1977.

[56] W. Freude, "Monomode operation of direct modulated GaAlAs DHS injection lasers from 260 Mbit/s up to 1.4 Gbit/s," *Arch. Elek. Übertragung.*, vol 32, pp. 105–110, Mar. 1978.

[57] C Baak, G. Elze, B. Enning, and G. Walf, "Modulation behaviour in the Gbit/s range of several GaAlAs lasers," *Frequenz*, vol. 32, pp. 346–350, Dec. 1978.

[58] C. Lindström, P. Tihanyi, T. Andersson, and P. Torphammar, "High bit rate modulation of narrow-stripe proton-implanted GaAs/GaAlAs injection lasers," *Electron. Lett.*, vol. 16, pp. 575–577, July 1980.

[59] R. Tell and S. T. Eng, "8 Gbit/s optical transmission with TJS laser and p-i-n detection," *Electron. Lett.*, vol. 16, pp. 497–498, June 1980.

[60] J.-I. Yamada, M. Saruwatari, K. Asatani, H Tsuchiya, A Kawana, K. Sugiyama, and T. Kimura, "High-speed optical pulse transmission at 1.29-μm wavelength using low-loss single-mode fibers," *IEEE J Quantum Electron.*, vol. QE-14, pp. 791–799, Nov. 1978.

[61] J.-I. Yamada, S. Machida, T. Mukai, H. Kano, and K. Sugiyama, "Modulation characteristics of 1.3-μm buried-stripe InGaAsP laser up to 2 Gbit/s data rates," *Electron Lett.*, vol 15, pp. 596–597, Sept. 1979.

[62] J.-I. Yamada, S. Machida, and T. Kimura, "2 Gbit/s optical transmission experiments at 1.3 μm with 44 km single-mode fibre," *Electron. Lett.*, vol. 17, pp. 479–480, June 1981.

[63] T. Ikegami, "Spectrum broadening and tailing effect in directly modulated injection lasers," in *Proc. 1st Europ. Conf. Optical Fibre Communication*, (London), paper 111, Sept. 1975.

[64] W Harth, "Properties of injection lasers at large-signal modulation," *Arch. Elek. Übertragung.*, vol. 29, pp. 149–152, Apr. 1975.

[65] K. Petermann and H. Storm, "Nichtlineare Verzerrungen bei der Modulation von Halbleiterlasern," *Wissenschaftliche Berichte AEG-Telefunken*, vol. 52, pp. 238–242, 1979.

[66] H. Storm, "Rauschen und Klirren beim V-Nut-Laser," *Wissenschaftliche Berichte AEG-Telefunken*, vol 53, pp. 23–26, 1980.

[67] G. Grosskopf and L. Küller, "Measurement of nonlinear distortions in index- and gain-guiding GaAlAs lasers," *J. Optical Communications*, vol. 1, pp. 15–17, 1980.

[68] D. E. McCumber, "Intensity fluctuations in the output of CW oscillators," *Phys. Rev.*, vol. 141, pp. 306–322, Jan. 1966.

[69] D. J. Morgan and M. J. Adams, "Quantum noise in semiconductor lasers," *Phys. Status Solidi*, vol. 11, pp. 243–253, 1972.

[70] T. Ito, S. Machida, K Nawata, and T Ikegami, "Intensity fluctuations in each longitudinal mode of a multimode AlGaAs laser," *IEEE J. Quantum Electron.*, vol. QE-13, pp. 574–579, Aug 1977.

[71] G. Arnold and K. Petermann, "Intrinsic noise of semiconductor lasers in optical communication systems," *Optical and Quantum Electronics*, vol. 12, pp. 207–219, 1980.

[72] J. W. M Biesterbos and A. J. Den Boef, "High-frequency noise in the output of DH(AlGa)As injection lasers with different structures and waveguiding mechanisms," *IEEE J. Quantum Electron.*, vol. QE-17, pp. 701–706, May 1981.

[73] N G Basov, "Dynamics of injection lasers," *IEEE J Quantum Electron.*, vol. QE-4, pp. 855–864, Nov. 1968.

[74] K. Kobayashi, "An analysis of pulsation in coupled cavity structure semiconductor lasers," *IEEE J. Quantum Electron.*, vol. QE-9, pp. 449–458, Apr. 1973.

[75] G. Arnold and K. Petermann, "Self-pulsing phenomena in (GaAl)As double-heterostructure injection lasers," *Optical and Quantum Electronics*, vol. 10, pp. 311–322, 1978.

[76] C. H. Henry, "Theory of defect-induced pulsations in semiconductor injection lasers," *J. Appl. Phys.*, vol. 51, pp. 3051–3061, 1980.

[77] W. Harth, "Diffusion induced instability in injection lasers," *Arch. Elek. Übertragung.*, vol. 36, pp. 136–137, Mar. 1982.

[78] T. Morikawa, Y. Mitsubishi, and J. Shimada, "Return-beam-induced oscillations in self-coupled semiconductor lasers," *Electron. Lett.*, vol. 12, pp. 435–436, Aug. 1976.

[79] O. Hirota and Y. Suematsu, "Noise properties of injection lasers due to reflected waves," *IEEE J. Quantum Electron.*, vol. QE-15, pp. 142–149, Mar. 1979.

[80] T. Kanada and K. Nawata, "Injection laser characteristics due to reflected optical power," *IEEE J. Quantum Electron.*, vol. QE-15, pp 559–565, July 1979.

[81] C. Baack, G. Elze, B. Enning, and G. Walf, "Modal noise and optical feedback in high-speed optical systems at 0.85 μm," *Electron. Lett.*, vol. 16, pp. 592–593, July 1980.

[82] R. Lang and K. Kobayashi, "External optical feedback effects on semiconductor injection laser properties," *IEEE J. Quantum Electron.*, vol. QE-15, pp. 142–149, March 1979.

[83] K. Petermann, "Gain- and index-guided injection lasers for wideband communication," in *Proc. 7th Europ. Conf. Optical Communication*, (Copenhagen), paper 10.1, Sept. 8–11, 1981.

[84] G. Arnold, "Influence of optical feedback on the noise behaviour of injection lasers," in *Proc. 7th Europ. Conf. Optical Communication*, paper 10.4, Sept. 8–11, 1981.

[85] P. Russer, "Modulation behaviour of injection lasers with coherent irradiation into their oscillating mode," *Arch. Elek. Übertragung.*, vol. 29, pp. 231–232, May 1975.

[86] R. Land and K. Kobayashi, "Suppression of relaxation oscillation in semiconductor lasers," presented at IEEE/OSA Conf. on Laser Engineering and Applications, Washington, DC, May 28–30, 1975.

[87] H. Hillbrand and P. Russer, "Large-signal p.c.m. behaviour of injection lasers with coherent irradiation into one of their oscillating modes," *Electron. Lett.*, vol. 11, pp. 372–374, Aug. 1975.

[88] R. Lang and K. Kobayashi, "Suppression of the relaxation oscillation in the modulated output of semiconductor lasers," *IEEE J. Quantum Electron.*, vol. QE-12, pp. 194–199, Mar. 1976.

[89] K. Otsuka, "Analysis of the effects of external injection and diffusion excited states on relaxation oscillations in lasers," *IEEE J. Quantum Electron.*, vol. QE-13, pp. 520–525, July 1977.

[90] G. Arnold, K. Petermann, P. Russer, and F.-J. Berlec, "Modulation behaviour of double heterostructure injection lasers with coherent light injection," *Arch. Elek. Übertragung.*, vol. 32, pp. 129–136, Apr. 1978.

[91] S. Kobayashi and T. Kimura, "Injection locking characteristics of an AlGaAs semiconductor laser," *IEEE J. Quantum Electron.*, vol. QE-16, pp. 915–917, Sept. 1980.

[92] S. Kobayashi, J. Yamada, S. Machida, and T Kimura, "Single-mode operation of 500 Mbit/s modulated AlGaAs semiconductor laser by injection locking," *Electron. Lett.*, vol. 16, pp. 746–747, Sept. 1980.

[93] B. G. Bosch, "Gigabit Electronics," in *Proc. 7th Europ. Microwave Conf.*, (Copenhagen), Sept. 5–8, 1977, pp. 393–402.

[94] J. B. Coughlin, R. G. Harbott, J. B. Hughes, and F. W. Siegert, "Circuit techniques for gigabit/s digital communication systems," in *Proc. 7th Europ. Microwave Conf.*, (Copenhagen), Sept. 5–8, 1977, pp. 532–536

[95] R. Petschacher and P. Russer, "Demultiplexer using fast hybrid integrated ECL-gates for 1 Gbit/s PCM systems," in *Proc. 7th Europ. Microwave Conf.*, (Copenhagen), Sept. 5–8, 1977, pp. 527–531.

[96] J. Gruber, P. Marten, R. Petschacher, and P. Russer, "Electronic circuits for high bit rate digital fiber optic communication systems," *IEEE Trans. Communications*, vol. COM-26, pp. 1088–1098, July 1978.

[97] J. Gruber, M. Holz. P. Marten, R. Petschacher, and E. Weidel, "A 1 Gbit/s fibre optic communications link," in *Proc. 4th Europ. Conf Optical Communication*, (Geneva), pp. 556–563, Sept 12–15, 1978

[98] J. Gruber, M. Holz, R. Petschacher, P. Russer, and E. Weidel, "Digitale Lichtleitfaser-Übertragungsstrecke für 1 Gbit/s," *Wissenschaftliche Berichte AEG-Telefunken*, vol. 52, pp. 123–130, 1979.

[99] G. Hanke, "Hybrid-integrated series to parallel converters for gigabit rates," *Electrocomponent Science and Technology*, vol. 4, pp. 57–62, 1977.

[100] F. Meyer, "Base-coupled logic circuits for high-speed digital systems," *Nachrichtentech. Z.*, vol. 29, pp. 828–830, Sept. 1976.

[101] W. Filensky, H.-J. Klein, and H. Beneking, "The GaAs MESFET as a pulse regenerator, amplifier, and laser modulator in the Gbit/s range," *IEEE J. Solid-State Circuits*, SC-vol 12, pp. 276–280, June 1977.

[102] K. Mause, A. Schlachetzki, E. Hesse, and H. Salow, "Gunn-device gigabit rate digital microcircuits," *IEEE J. Solid-State Circuits*, vol. SC-10, pp. 2–12, Feb. 1975.

[103] P. Russer and J. Gruber, "Hybrid integrierter Multiplexer mit Speicherschaltdioden für den Gbit/s-Bereich," *Wissenschaftliche Berichte AEG-Telefunken*, vol. 48, pp. 55–60, 1975.

[104] U. Barabas, U. Wellens, U. Langmann, and B. G. Bosch, "Diode circuits for pulse regeneration and multiplexing at ultrahigh bit rates," *IEEE Trans. Microwave Theory Tech.* MTT-24, pp. 929–935, Dec. 1976.

[105] U. Barabas, U Langmann, and B. G. Bosch, "Diode multiplexer in the multi-Gbit/s range," *Electron. Lett.*, vol. 14, pp. 62–64, 1978.

[106] R. Schwarte, B. Brinkmeier, J. Fischer, H. Koppenhöfer, K. H.

Narzinski, and R. Sinning, "Theoretical and experimental results of a distributed serial to parallel and parallel to serial converter for gigabit rates," in *Proc. 7th Europ. Microwave Conf.*, (Copenhagen), Sept. 5–8, 1977, pp. 537–541.

[107] R. E. Epworth, "Subsystems for high-speed optical links," in *Proc. 2nd Europ. Conf. Optical Fiber Communication*, (Paris), Sept. 27–30, 1976, pp. 377–382.

[108] P. W. Shumate and M. DiDomenico, "Light-wave transmitters," *Topics in Applied Physics*, vol. 39, pp. 161–200, 1982.

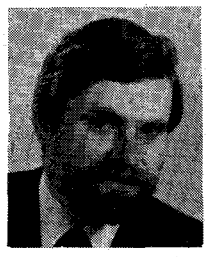

Peter Russer (SM'81) was born in Vienna, Austria, in 1943. He received the Dipl. Ing. degree in 1967 and the Dr. Techn. degree in 1971, both in electrical engineering and both from the Vienna Technical University, Vienna, Austria.

From 1968 to 1971 he was an Assistant Professor at the Institute of Physical Electronics of the Vienna Technical University, where he carried out research work on the Josephson effect. In 1971 he joined the Research Institute of AEG-Telefunken, Ulm, Germany, where he worked on fiber optic communication, high-speed solid-state electronic circuits, laser modulation, and fiber optic gyroscopes. He was corecipient of the NTG-award (1979). Since January 1981 he has held the Chair of High Frequency Engineering at the Technical University Munich, Germany. His current research interests are Josephson effect and optical communications.

Prof. Russer is a member of the Austrian Physical Society (OPG), the German Physical Society (DPG), and the Nachrichtentechnische Gesellschaft (NTG), Germany.

Günther Arnold was born in Jena, Germany, on April 7, 1932. He received the Dipl. Phys. degree in physics from the University of Jena, Germany, in 1958, and the Dr.Rer.Nat. degree from the University of Ulm, Germany, in 1976.

From 1958 to 1960 he was responsible for the spectroscopy laboratory at Light & Co., Colnbrook, England. From 1960 to 1964 he was a member of the Max Planck Institut für Spektroskopie, Göttingen, Germany, and worked on reaction kinetics and molecular spectroscopy. In 1965 he joined the Research Institute of AEG-Telefunken in Ulm, Germany. After structural research work on UV-sensitive films for optical data storage, he joined the optical communication group in 1973 and is engaged in research work on semiconductor laser properties.

An Exact Analysis of Group Velocity for Propagation Modes in Optical Fibers

KATSUMI MORISHITA, MEMBER, IEEE, YOSHIO OBATA, AND NOBUAKI KUMAGAI, FELLOW, IEEE

Abstract—**A method for calculating exactly the group velocity of propagation modes in optical fibers is proposed. In this analysis, optical fibers can contain uniaxial and dispersive media. The group velocity obtained by using the scalar approximate analysis is compared numerically with the rigorous group velocity computed by this method for square-law index optical fibers.**

I. Introduction

THE SCALAR approximation method is one of the most widely used techniques in optical fiber analysis because of short computing time and simple treatment. The method, however, has much error in the near cutoff region [1], [2], and the inaccuracies of group velocity are of practical importance for the analysis of pulse broadening, particularly in optical fibers which have few propagation modes. A method is needed for calculating exactly the group velocity of propagation modes in various optical fibers. There are several approximate methods giving the group velocity, i.e., a computational method based on the WKB theory [3], a method using the scalar finite-element analysis [4], a practical method using the scalar multilayer analysis [5], and a method with the vector multilayer analysis and the integral expression for the group velocity in the scalar analysis [6]. Kharadly [7] calculated the exact group velocity of the dielectric-tube waveguides constituted by three layers without material dispersion. To the authors' knowledge, however, a practical method giving the exact group velocity has not yet been proposed.

It is the purpose of this paper to describe a method for computing rigorously the group velocity of propagation modes in optical fibers without numerical differentiation, including uniaxial and dispersive material. The group velocity is determined by using the vector multilayer approximation and the integral expression for the group velocity in vector analysis. The calculated results have only the error caused by the multilayer approximation of index distribution, and are exact for the staircase index optical

Manuscript received March 16, 1982; revised July 16, 1982.

K. Morishita is with the Department of Precision Engineering, Osaka Electro-Communication University, Neyagawa, Osaka 572, Japan.

Y. Obata is with Kansai Electric Power Company, Osaka, Japan.

N. Kumagai is with the Department of Electrical Communication Engineering, Osaka University, Osaka 565, Japan.

0018-9480/82/1100-1821$00.75 ©1982 IEEE